Chemistry of Thiophene on ZnO, S/ZnO, and Cs/ZnO Surfaces: Effects of Cesium on Desulfurization Processes

Tomas Jirsak, Joseph Dvorak, and José A. Rodriguez*

Department of Chemistry, Brookhaven National Laboratory, Upton, New York 11973

Received: March 26, 1999; In Final Form: May 7, 1999

The adsorption of thiophene (C_4H_4S) on clean ZnO and oxide surfaces precovered with S and Cs has been studied using synchrotron-based high-resolution photoemission and ab initio self-consistent-field (SCF) calculations. On polycrystalline ZnO, C_4H_4S is weakly chemisorbed, and most desorbs at temperatures below 250 K. A very small fraction of the adsorbed C_4H_4S (∼0.02 monolayer) that interacts with O-unsaturated Zn sites decomposes on the oxide surface. S adatoms weaken the bonding interactions of thiophene on ZnO, whereas Cs adatoms enhance the adsorption energy of the molecule by at least 5−10 kcal/mol and facilitate the cleavage of C−S bonds. Pure metallic Cs reacts vigorously with C_4H_4S, decomposing the molecule at very low temperatures (100−200 K). The Cs atoms supported on ZnO are in an ionic state ($Cs^{\delta+}$), but they retain a large chemical affinity for thiophene. Small amounts of Cs (∼0.2 monolayer) are enough to activate the oxide surface. Results of ab initio SCF calculations indicate that the bonding interactions of thiophene with the (0001)-Zn and (000$\bar{1}$)-O faces of ZnO are weak, and promotion with Cs adatoms considerably improves the energetics for C_4H_4S adsorption and C−S bond breaking. The Cs adatoms provide occupied states that are very efficient for bonding interactions with the frontier orbitals of C_4H_4S and other S-containing molecules. This should lead to an improvement in the performance of ZnO as a sorbent in desulfurization processes.

I. Introduction

Most of the petroleum used nowadays in refineries for the production of fuels and chemical feedstocks contains a significant amount of organosulfur molecules.[1] These S-containing molecules constitute a major problem. On one hand, they poison catalysts used in the petrochemical industry for the re-forming of hydrocarbons.[2] On the other hand, the S-containing molecules present in fuels react with oxygen during combustion processes producing SO_x species that constitute an environmental problem.[3] In the refineries a big effort is focused on the removal of the organosulfur molecules from the oil.[1] This involves two steps. First, the oil fractions undergo hydrodesulfurization (HDS) processes on Mo- and W-based catalysts.[4] The HDS processes are not 100% effective, and the oil-derived feedstocks are then passed over sorbents.[1,5] Zinc oxide is used as a sorbent in many refineries, and there is a general desire to improve its performance in the removal or destruction of S-containing molecules.[1,5] In particular, when dealing with the sorption of organosulfur molecules that have a relatively high stability and exhibit weak interactions with the oxide like thiophenes.[5]

Thiophene is a typical test molecule for desulfurization studies due to its low reactivity.[4−6] The surface chemistry of the molecule on metals has been extensively studied.[6b,7−16] Thiophene dissociatively adsorbs at 300 K on single-crystal surfaces of many transition metals (Mo,[7] W,[8] Re,[9] Fe,[10] Ni,[11] Ru,[12] Rh,[13] Pd,[14] Pt[15]) except Cu surfaces where the adsorption is molecular and reversible with no evidence for dissociation.[16] In these systems, the molecule can be bonded with its aromatic ring parallel to the surface[8,13,15,16b] or through the S end.[7,16a] Little is known about the interaction of thiophene with oxides.[17] On alumina, thiophene interacts only weakly with the substrate (desorption temperature < 250 K), and no decomposition of the molecule was observed.[17a] At saturation, three kinds of adsorbed thiophene species were found: one in which the thiophene interacts weakly with hydroxyl groups (probably through hydrogen bonding), a second in which thiophene is coordinated via its sulfur atom to coordinatively unsaturated Al^{3+} sites, and a third species with an unknown bonding configuration.[17a]

In this paper, we examine the adsorption of thiophene on pure and modified polycrystalline zinc oxide using synchrotron-based high-resolution photoemission and ab initio self-consistent-field (SCF) calculations. The effects of S and Cs on the surface chemistry of thiophene are examined. On ZnO sorbents, sulfur is present in the surface as a result of the adsorption and decomposition of mercaptans and disulfides.[5] On the other hand, previous studies[21,27] suggest that Cs should increase the reactivity of ZnO toward thiophene. Here, it is found that the Cs ↔ thiophene interactions are very strong, even when Cs is supported on ZnO in an ionic state ($Cs^{\delta+}$). Our results indicate that Cs adatoms should enhance substantially the efficiency of ZnO when dealing with the sorption of organosulfur molecules that interact weakly with the clean oxide.

II. Experimental and Theoretical Methods

II.1. Instrumentation and Sample Preparation. All the experiments were performed at the U7A beamline of the National Synchrotron Light Source (NSLS) at Brookhaven National Laboratory. The beamline is equipped with a toroidal-spherical grating monochromator that can deliver photons ranging in energy from 200 to 1200 eV. The ultrahigh-vacuum chamber (base pressure ∼ 5×10^{-10} Torr) in this beamline is fitted with a hemispherical electron-energy analyzer with multichannel detection, a Mg Kα X-ray source, low-energy

* To whom all the correspondence should be sent. FAX: (516) 344-5815. E-mail: rodrigez@bnl.gov.

10.1021/jp991051p CCC: $18.00
Published on Web 06/16/1999

electron-diffraction (LEED) optics, and a quadrupole mass spectrometer. Photoemission measurements were carried out at a photon energy of 380 eV (C 1s spectra, S 2p spectra, and valence band region). The Cs 3d X-ray photoelectron spectroscopy (XPS) data were taken with unmonochromatized Mg Kα radiation. The sample was positioned at a takeoff angle of 45° for both photoemission and XPS measurements. The binding energy (BE) scale in the spectra acquired using synchrotron radiation was calibrated by the position of the Fermi edge, while the BE scale in the experiments using the X-ray source was established by setting the Cs $3d_{5/2}$ peak of a thick Cs multilayer at a binding energy of 726.6 eV.[18]

Photoemission experiments were performed on ZnO, Cs/ZnO, S/ZnO, and ZnS surfaces. Polycrystalline surfaces of ZnO were prepared by vapor depositing Zn under an O_2 background ($\sim 1 \times 10^{-5}$ Torr) on a Mo(110) crystal at ~200 K, followed by annealing to 700 K.[19] This methodology leads to quasi layer-by-layer growth and ZnO films (>10 monolayers in thickness) that have electronic properties and a phonon structure identical to those of bulk zinc oxide.[19] Cesium was vapor deposited on the ZnO surfaces by heating a SAES getter chromate source.[21] For small doses, the relative coverage of Cs (θ_{Cs}) was determined by comparing the area under the Cs 3d XPS peaks to the corresponding area for a saturated layer of Cs on zinc oxide at 300 K ($\theta_{Cs} \sim 0.6$ monolayer).[21] ZnS films (>10 monolayer in thickness) were prepared by dosing of S_2 and Zn on the clean Mo(110) surface at 100 K with subsequent annealing to 750 K.[20] S_2 was generated in situ by decomposing Ag_2S in a solid-state electrochemical cell: Pt/Ag/AgI/Ag_2S/Pt.[22,23]

High-purity thiophene (Aldrich) was dosed to ZnO, Cs/ZnO, S/ZnO, and ZnS from the background by back-filling the chamber. The crystal remained at the photoemission position during gas dosing, and an increase of the pressure was measured by an ion gauge (exposures are expressed in langmuirs; 1 langmuir = 10^{-6} Torr·s^{-1}). A procedure of nonlinear least-squares fitting with an asymmetric Doniach−Sunjic function was used to quantify the S 2p and C 1s photoemission data,[25] and a linear background subtraction was performed before each fit. The S 2p and C 1s areas of adsorbed thiophene were scaled to absolute coverage values by comparing them to the corresponding area for 0.6 monolayer of S on ZnO.[24] In this work the coverages are reported with respect to the number of Mo(110) surface atoms ($\theta = 1$ monolayer corresponds to 1.43×10^{15} species cm^{-2}).

II.2. Theoretical Methods. Ab initio SCF calculations were used to examine the bonding interactions of thiophene with ZnO (section III.1) and Cs/ZnO (section III.3) clusters. The calculations were performed using the HONDO program.[26] The Zn, O, and Cs atoms were treated using the basis sets and effective-core potentials employed in our previous studies for the adsorption of H_2S, S_2, or SO_2 on ZnO and Cs/ZnO.[21a,24,27] The atoms in the thiophene molecule were described including all their electrons in the calculations, using 6-31G basis sets for C and S and a double-ζ quality basis augmented with polarization functions for H (4s1p/2s1p).[28] Previous experience[21a,24,27,29] indicates that the type of ab initio SCF calculations performed here give satisfactory adsorption geometries. Due to the approximations in our theoretical approach, the energetics derived from these SCF calculations simply provides a guide for the interpretation of the experimental results.[21a,24,27,29] The limited size of the basis sets and the lack of electron correlation introduce uncertainty in the computed bonding energies. Despite this limitation, the use of ab initio SCF methods with cluster models has proved to be a very useful approach for studying a large variety of phenomena that occur on surfaces of metals and oxides.[27−32]

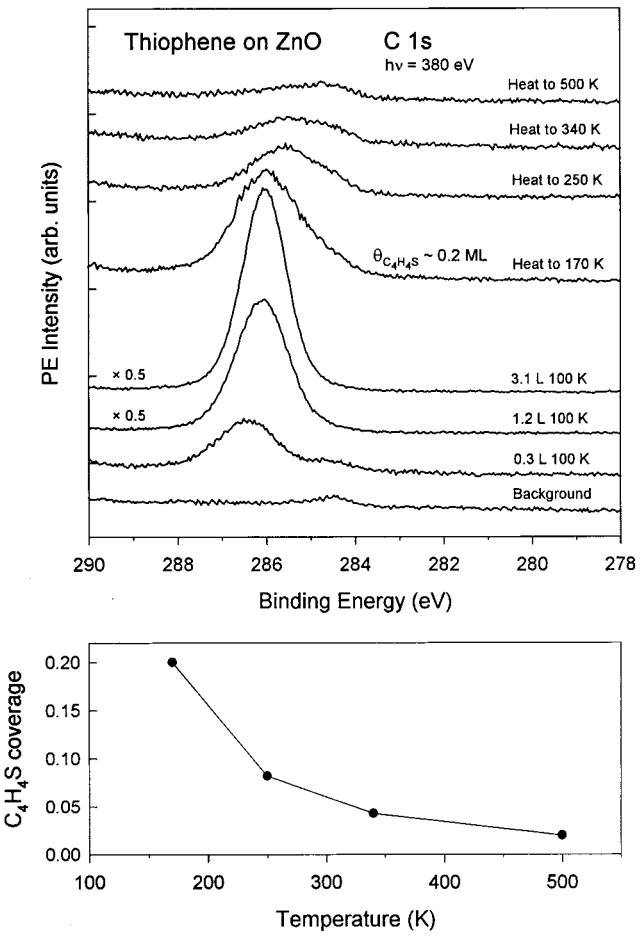

Figure 1. (Top panel) C 1s spectra for the adsorption of thiophene on a clean polycrystalline ZnO surface at 100 K, followed by annealing to 170, 250, 340, and 500 K (where ML = monolayer and L = langmuir). (Bottom panel) Coverage of thiophene as a function of annealing temperature. All the spectra were acquired in the same set of experiments that produced the S 2p spectra in Figure 2 using a photon energy of 380 eV.

III. Results

III.1. Adsorption of Thiophene on ZnO. The top panel of Figure 1 shows C 1s photoelectron spectra acquired after adsorption of thiophene on a clean polycrystalline ZnO surface at 100 K followed by annealing to elevated temperatures. The bottom spectrum shows that the ZnO surface is essentially carbon free before beginning the dosing of thiophene (a trace of carbon at a binding energy of 284.4 eV corresponds to less than 0.01 monolayer). The first dose produces a symmetric feature at a BE of 286.3 eV. It grows in intensity upon further dosing while its binding energy shifts to 286.0 eV. A final dose of 3.1 langmuir leads to a high-intensity peak, indicating condensation of thiophene in a physisorbed multilayer. Upon annealing to 170 K the multilayer desorbs[12,13,16a] leaving only chemisorbed species on the ZnO surface. At this point the coverage of thiophene is about 0.2 monolayer. A shoulder on the lower binding-energy side indicates that the molecule is adsorbed on more than one type of sites or bonding configurations. Further heating to 250 K induces desorption of most of the chemisorbed thiophene. The bottom panel in Figure 1 shows the thiophene coverage on the oxide surface as a function of

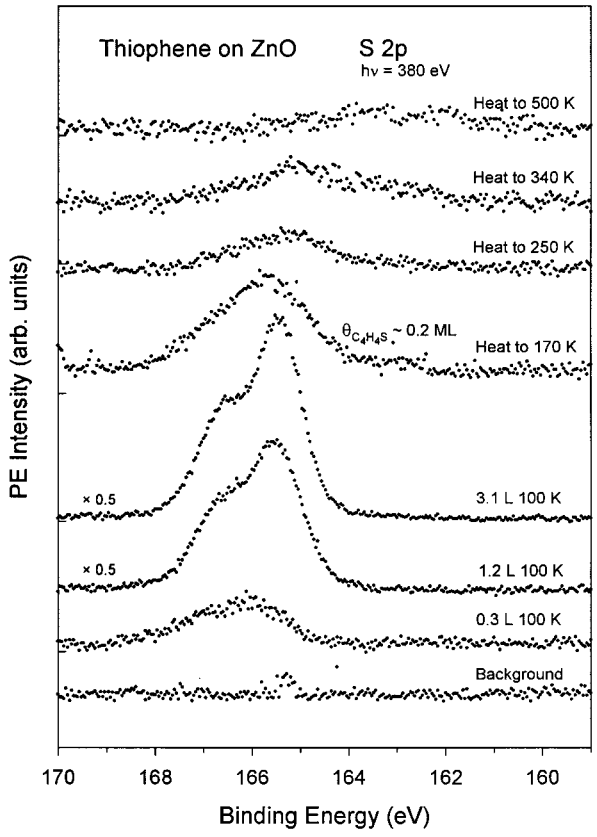

Figure 2. Sulfur 2p spectra for the adsorption of thiophene on a clean polycrystalline ZnO surface at 100 K, followed by annealing to 170, 250, 340, and 500 K (where ML = monolayer and L = langmuir). All the spectra were acquired in the same set of experiments that produced the C 1s spectra in Figure 1 using a photon energy of 380 eV.

the annealing temperature (the values were obtained after subtraction of the carbon amount in the background spectrum). It shows that thiophene desorbs from polycrystalline ZnO in a broad range of temperatures. The majority of the molecules (>70%) are weakly bonded, but some of them (<0.05 monolayer) exhibit adsorption energies in the range of 15−20 kcal/mol. The strongly bonded molecules were probably interacting with Zn sites that have a relatively low coordination number on the rough oxide substrate.

S 2p spectra, taken at the same stage of the experiments in Figure 1, are shown in Figure 2. After heating to 170 K, the thiophene multilayer desorbs and the S 2p signal for chemisorbed thiophene gradually diminishes during further annealing to 500 K. At the end, one sees a very weak S 2p signal between 162 and 164 eV, where atomic sulfur on ZnO appears.[24,33] S and C are stable on ZnO at temperatures well above 500 K.[23,24] By examining the C 1s and S 2p data, one can conclude that thiophene adsorbs on the ZnO surface molecularly at 100 K and most of it (~90%) completely desorbs upon heating to 500 K.

The bonding of thiophene to Zn sites of zinc oxide was examined using ab initio SCF calculations and the $Zn_{13}O_{13}$ cluster displayed in Figure 3. Previous studies (S_2/ZnO,[24] H_2S/ZnO,[27] HS/ZnO,[27] SO_2/ZnO[33]) have shown that this cluster provides the basic bonding interactions between S-containing molecules and zinc oxide. The $Zn_{13}O_{13}$ cluster has four layers arranged in the structural geometry of bulk ZnO.[34] The first and third layers are entirely zinc, and the second and fourth are oxygen layers. The atoms in the first layer can be used to model tri- and di-coordinated zinc atoms (Zn_1 and Zn_2, respectively) of zinc oxide. The C_4H_4S molecule was bonded to Zn_1 and Zn_2

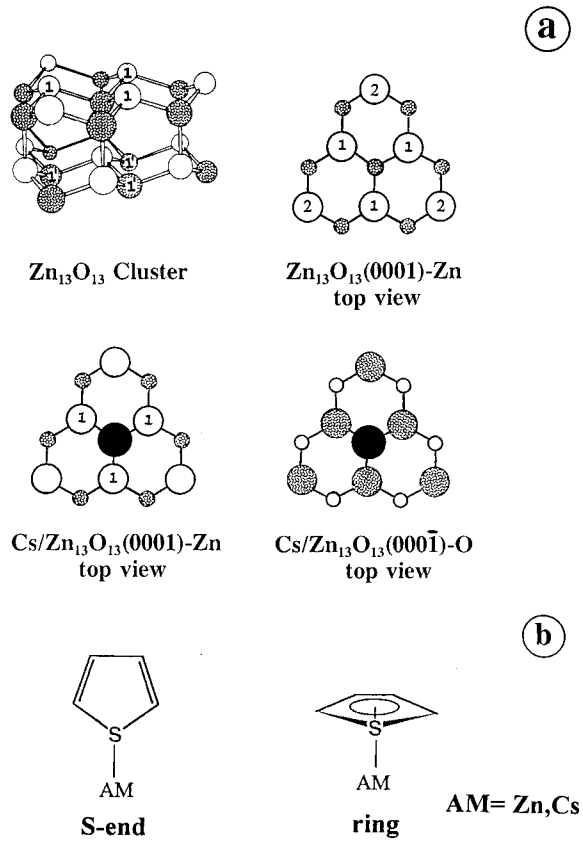

Figure 3. (a) Cluster used to model the adsorption of C_4H_4S on ZnO and Cs/ZnO surfaces. The cluster has 13 zinc atoms (empty circles) and 13 oxygen atoms (shaded circles) arranged in four layers with the geometry reported for the bulk oxide.[34] The (0001)-Zn and $(000\bar{1})$-O faces of zinc oxide are represented by the first and four layers, respectively. A Cs atom was set directly above the hollow site formed by the Zn_1 atoms in the first layer {$Cs/Zn_{13}O_{13}$(0001) configuration} or above the hollow site formed by the $O_{1'}$ atoms in the fourth layer {$Cs/Zn_{13}O_{13}(000\bar{1})$ configuration}. (b) Bonding geometries for the adsorption of thiophene on Zn and Cs atoms of ZnO and Cs/ZnO. The molecule was bonded to a Zn_1 or Zn_2 atom of the $Zn_{13}O_{13}$(0001) system or to the supported Cs atom in the $Cs/Zn_{13}O_{13}$(0001) and $Cs/Zn_{13}O_{13}$-$(000\bar{1})$ systems.

sites of the $Zn_{13}O_{13}$ cluster in the two coordination modes displayed at the bottom of Figure 3: via the S atom or through the aromatic ring. These are the two bonding configurations most frequently observed for the molecule in organometallic complexes and metal surfaces.[6,7]

Table 1 lists bonding energies and structural parameters calculated for the $C_4H_4S/Zn_{13}O_{13}$ system. The adsorption energies predicted in our SCF calculations (2−6 kcal/mol) are smaller than those observed experimentally. This, in part, can be attributed to a lack of electron correlation in our theoretical approach.[30a,b,31] In the past, we have found that this is not a serious deficiency if one is interested in qualitative trends.[21,24,27−29,33] On a tri-coordinated Zn_1 site, the bonding energies for adsorption of thiophene through the S-end or the ring are very similar. A Zn_1 site is missing only one neighbor to achieve tetrahedral coordination and thus prefers to interact with C_4H_4S via the S lone pairs of the molecule. In the case of a di-coordinated Zn_2 atom, adsorption through the ring is clearly more stable than via the S-end. This agrees with previous experimental and theoretical studies,[6a,28,36] which show that thiophene prefers to adopt a ring coordination when bonded to metal atoms that have a low coordination number in organometallic complexes and sulfides.

TABLE 1: Adsorption of Thiophene on $Zn_{13}O_{13}$

	ads energy[a] (kcal/mol)	bond distances (Å)				thiophene charge (e)
		Zn−S	Zn−C	C−S	C−C	
free molecule				1.78	1.34	
on Zn_1(tri-coordinated)						
S-end[b]	3	2.48		1.78	1.34	0.08
ring[b]	2	2.56	2.47	1.78	1.34	0.01
on Zn_2 (di-coordinated)						
S-end[c]	3	2.46		1.78	1.34	0.09
ring[d]	6	2.51	2.39	1.79	1.34	0.04

[a] A positive value denotes an exothermic process. [b] The molecular plane of thiophene was either perpendicular (S-end adsorption) or parallel (ring adsorption) to the (0001)-Zn terminated face of the cluster. In both configurations, the adsorbate cluster interactions were weak and there was essentially no barrier for the rotation of the molecular plane around the (0001) surface normal. [c] The molecular axis of thiophene was in the plane that contained the two Zn_2−O bonds (two identical S−Zn_2−O angles in the system). [d] In the adsorption complex, the σ_v plane of the molecule (perpendicular to the aromatic ring) also contained the two Zn_2−O bonds.

After optimizing the geometry of free thiophene at the ab initio SCF level, we found bond distances (C−S = 1.78 Å; C−C = 1.34 Å; C−C = 1.45 Å) and bond angles that are very close to those observed in experiments of electron diffraction.[35] The adsorption process produced almost no change in the geometry of the molecule (see Table 1), even when thiophene was bonded to a di-coordinated Zn_2 site. Therefore, it is not surprising the lack of decomposition seen in the experimental results for thiophene on ZnO (Figures 1 and 2). Due to their low electron density, the metal cations in ZnO are not able to donate electrons into the LUMO of thiophene. An increase in the electron population of this molecular orbital, which is C−S antibonding,[28] facilitates the dissociation of thiophene on metals and sulfides.[28,36]

III.2. Adsorption of Thiophene on ZnS and S/ZnO. In industrial operations, thiophenes interact with ZnO surfaces which contain sulfur adatoms produced by the decomposition of other S-containing molecules that have a high chemical reactivity.[5] In this section, we examine the adsorption of thiophene on ZnS and S/ZnO (θ_S = 0.2 monolayer) at 100 K. The chemistry of thiophene on ZnS is quite simple as the C 1s spectra show in Figure 4. Dosing of thiophene and subsequent annealing produces only one peak at a BE of ∼285.8 eV. Its intensity grows with exposure of thiophene. When the surface is annealed to 170 K, one sees a significant drop in intensity caused by desorption of the physisorbed multilayer.[12,13,16a] Only a chemisorbed overlayer with a thiophene coverage of ∼0.1 monolayer remains on the surface. The thermal stability of the chemisorbed overlayer is low, and annealing to 270 K leads to a clean ZnS surface with no carbon. A comparison of the results in Figures 1 and 4 indicates that the thiophene bonding interactions are considerably stronger on ZnO than on ZnS.

The adsorption properties of thiophene on $S_{0.2}$/ZnO are shown in Figure 5. The C 1s spectrum at the bottom was taken before beginning the dosing of thiophene and demonstrates that no carbon impurities were present on the $S_{0.2}$/ZnO surface. An initial dose of 0.2 langmuir produces a carbon feature at a BE of ∼286.5 eV. It grows upon additional doses. Annealing to 170 K leaves only a chemisorbed thiophene overlayer (∼0.2 monolayer) which almost completely desorbs after further heating to 250 K. The presence of sulfur on the surface leads to a lower desorption temperature of thiophene in comparison with ZnO (Figure 1). At 250 K the amount of atomic sulfur in the $C_4H_4S/S_{0.2}$/ZnO system was about the same as at the beginning of the experiment (i.e. ∼0.2 monolayer). Thus, thiophene essentially adsorbs and desorbs nondissociatively on a $S_{0.2}$/ZnO surface.

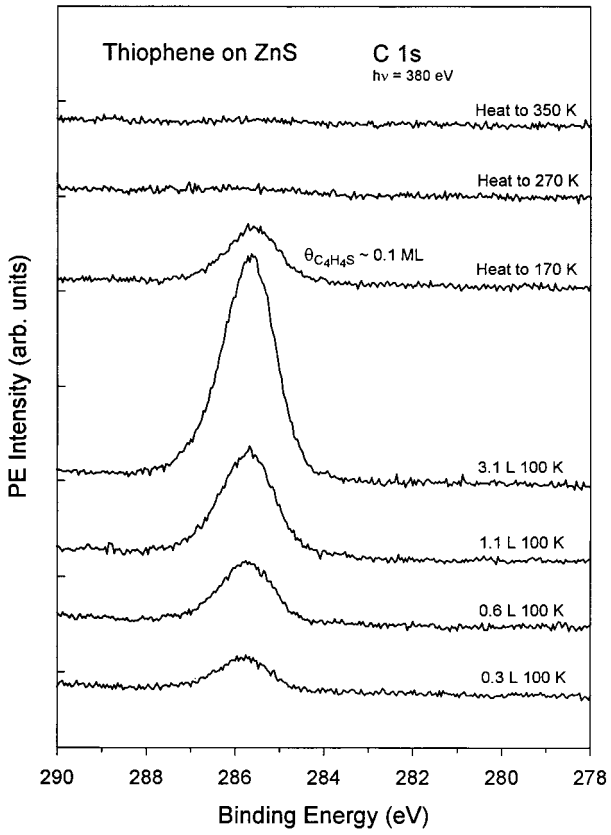

Figure 4. Carbon 1s spectra obtained after exposing a clean polycrystalline ZnS surface to repeated thiophene doses at 100 K, followed by annealing to 170, 270, and 350 K (where ML = monolayer and L = langmuir). All the spectra were acquired using a photon energy of 380 eV.

III.3. Adsorption of Thiophene on Metallic Cs and Cs/ZnO. Before studying the adsorption of thiophene on Cs/ZnO surfaces, it is worthwhile to examine the interaction of the molecule with pure metallic Cs. Figure 6 presents S 2p photoemission spectra acquired after the adsorption of thiophene on a thick (>6 monolayers) Cs layer at 100 K. Due to the high reactivity of cesium and the presence of sulfur-containing species in the residual atmosphere of the experimental chamber, the background spectrum shows already a weak feature at a BE of ∼161 eV, which is also seen after deposition of pure sulfur on metallic Cs.[27] Dosing of 1.5 langmuirs of thiophene produces several species in the S 2p region between 163 and 169 eV while the amount of atomic sulfur (∼161 eV) remains about the same. The feature at a BE of 167.3 eV grows after another dose of 2.5 langmuirs (and during further dosing, not shown) and corresponds to a physisorbed thiophene multilayer. By comparing the spectra as a function of dosing, one sees that the other features at BE's of 166 and 163.8 eV are essentially saturated by the first dose. The former one is characteristic of molecular thiophene and was also seen on ZnO and ZnS (see above); the latter one corresponds to partially decomposed thiophene (C_xH_yS, it can involve only one C−S bond). When the sample is annealed to 170 K, the physisorbed thiophene desorbs and the intensities of both molecular and partially decomposed thiophene (BE's of 166 and 163.8 eV) do not change. Further annealing to 250 K produces dramatic changes in the line shape: (i) the molecular thiophene peak substantially decreases, (ii) a new species appears at a BE of 165 eV, and

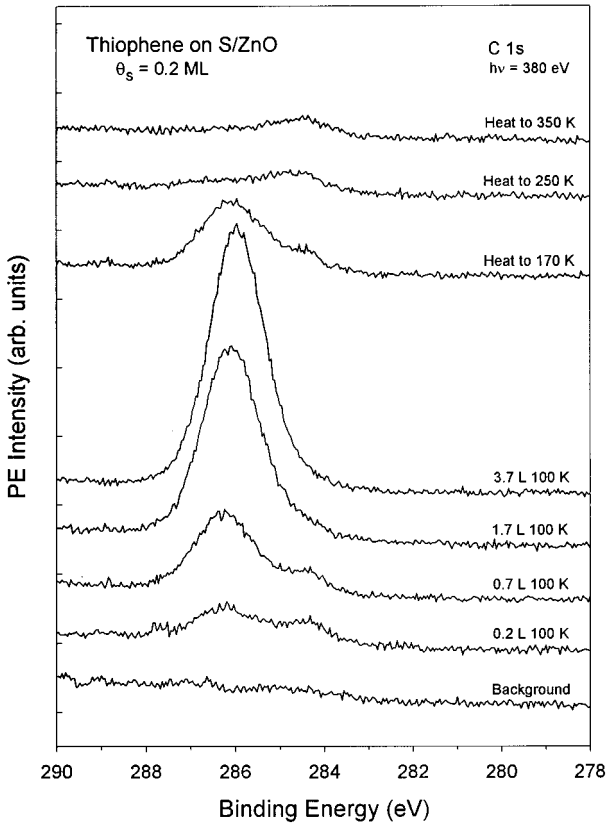

Figure 5. C 1s spectra for the adsorption of thiophene on S/ZnO (θ_S = 0.2 monolayer) at 100 K and after annealing to 170, 250, and 350 K (where ML = monolayer and L = langmuir). All the spectra were obtained using a photon energy of 380 eV.

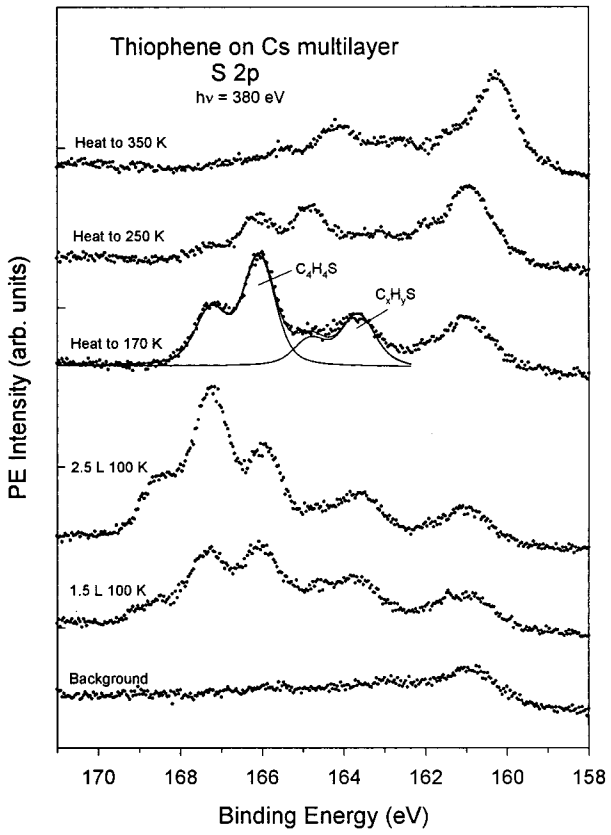

Figure 6. Sulfur 2p spectra for thiophene dosed on a Cs multilayer at 100 K and subsequent annealing to 170, 250, and 350 K(where L = langmuir). All the spectra were acquired in the same set of experiments that produced the C 1s spectra in Figure 7 using a photon energy of 380 eV.

(iii) the intensity of the atomic-sulfur feature (161 eV) increases. During heating part of the thiophene desorbs, but a significant fraction of the adsorbed molecules undergoes C−S bond cleavage between 170 and 250 K. The annealing to 350 K induces a −0.8 eV shift in the binding energies of all the photoemission peaks including those in the C 1s region (see below). Such behavior, which has also been observed for the SO_2/Cs[21a] and O_2/Cs[38] systems, suggests the occurrence of a phase transition or transformation that shifts the position of the Fermi edge for the film.[39] After the final heating to 350 K, atomic S bonded to cesium is the dominant sulfur species present in the system.

The corresponding C 1s spectra shown in Figure 7 also yield a complex picture for the reaction of thiophene with metallic Cs. Upon the initial dose of 1.5 langmuirs at 100 K, a very broad feature appears between 284 and 289 eV. It is well-fitted with three peaks positioned at the BE's of 287.8, 286.9, and 285.8 eV. The first and weakest feature further grows after the next dose of 2.5 langmuirs and disappears upon heating to 170 K. It clearly corresponds to a physisorbed thiophene multilayer. The spectrum taken after annealing to 170 K can be fitted with two peaks at BE's of 286.8 and 285.9 eV, representing chemisorbed and partially decomposed thiophene, respectively. Further heating to 250 K leads to a substantial decrease of the molecular thiophene feature. In the temperature range of 170−350 K, adsorbed thiophene desorbs or decomposes on the surface.

Figure 8 shows Cs 3d XPS data acquired after dosing thiophene to a polycrystalline Cs film at 100 K, followed by successive annealing to 180 and 250 K. For the Cs multilayer, the two sharp features at 726.6 and 740.5 eV are the main 3d levels, whereas the broad shoulders toward higher binding energy correspond to plasmon loses.[27,37] At the beginning of the dosing, the reaction with thiophene leads to a gradual decrease in the magnitude of the plasmon loses, with the main 3d levels gaining intensity. The large doses (2 and 4 langmuirs) produce a thick physisorbed thiophene overlayer which attenuates the signal coming from the underlying cesium. When the sample is annealed from 100 to 180 K, the thick thiophene multilayer desorbs and the Cs 3d signal gains intensity back. Upon annealing to 250 K, the Cs 3d peaks shifts ∼0.5 eV to lower binding energy. This behavior is similar to that observed during the reaction of metallic cesium with SO_2[21a] and S_2[27] and corresponds to the formation of a CsS_x compound.

The photoemission results in Figures 6−8 indicate that metallic cesium reacts vigorously with thiophene. Thus, in principle, Cs adatoms could be effective for enhancing the reactivity of oxide surfaces toward thiophene. This hypothesis, however, may not hold due to the strong bonding interactions between Cs and oxide surfaces[41] that can induce substantial changes in the chemical activity of the alkali metal. The interaction of cesium with polycrystalline ZnO was examined in detail in a previous work.[42] At small coverages, $\theta_{Cs} \leq 0.2$ monolayer, cesium forms very strong adsorption bonds (desorption temperatures > 700 K) and the adatoms are in a highly ionic state but not fully oxidized ($Cs^{\delta+}$).[42] As the Cs coverage increases, there is a decrease in the ionic character of the alkali metal−oxide bond and the admetal desorbs at lower temperatures: 500−700 K.[42] For a saturated adlayer ($\theta_{Cs} \approx 0.6$ monolayer) the desorption on the alkali metal starts around 300 K.[42] In this work, we examined the adsorption of thiophene on ZnO surfaces precovered with 0.4 and 0.2 monolayer of cesium ($Cs_{0.4}$/ZnO and $Cs_{0.2}$/ZnO, respectively).

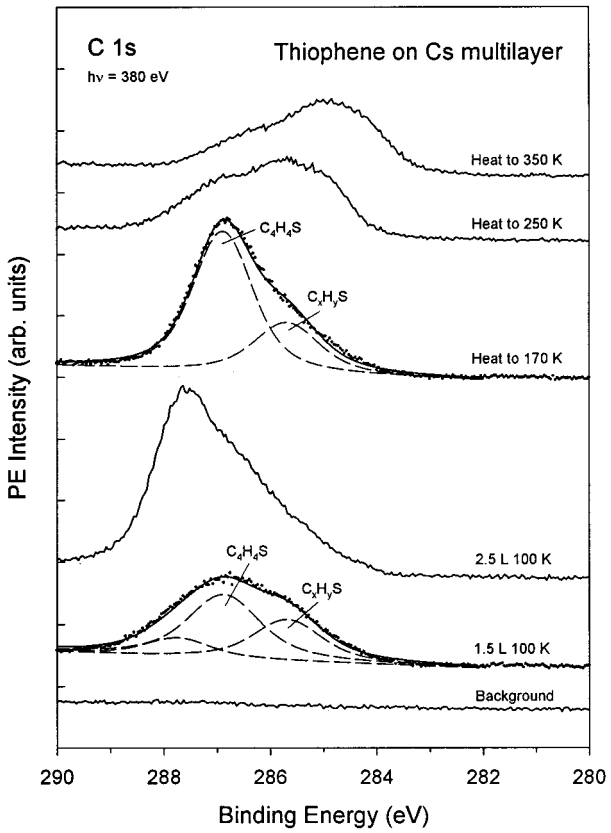

Figure 7. Carbon 1s spectra for thiophene dosed on a Cs multilayer at 100 K and subsequent annealing to 170, 250, and 350 K (where L = langmuir). All the spectra were acquired in the same set of experiments that produced the S 2p spectra in Figure 6 using a photon energy of 380 eV.

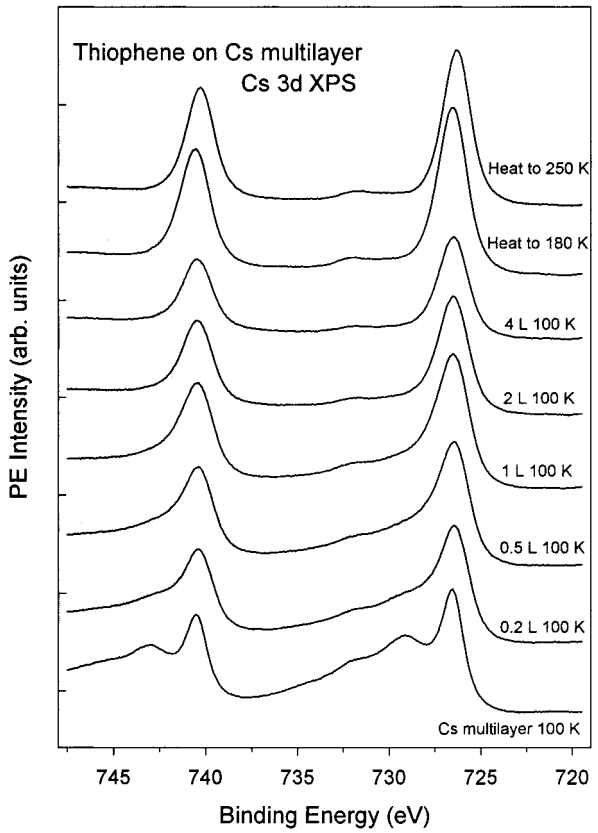

Figure 8. Cs 3d XPS spectra for C_4H_4S/cesium as a function of thiophene exposure at 100 K and annealing to 180 and 250 K (where L = langmuir). These spectra were acquired using Mg Kα radiation.

In Figure 9, the C 1s and S 2p results are displayed for the $Cs_{0.4}$/ZnO system upon thiophene adsorption at 100 K followed by annealing. The weak features at 159−162 eV appear before beginning of the dosing (adsorption of S species from the background) at a position found after deposition of sulfur on metallic Cs.[27] For the lowest thiophene exposure of 0.2 langmuir, one sees small features in both the C 1s and S 2p regions at BE's of 286.5 and 166 eV. Upon dosing 0.7 langmuir of thiophene, the spectrum for the S 2p levels shows a growth between 165 and 169 eV and no change in intensity of the atomic sulfur centroid at 160.5 eV. The features between 165 and 169 eV can be fitted with two doublets at BE's of 165.7 and 166.5 eV. The feature at 165.7 eV saturates after a dose of 1.2 langmuirs, while the doublet at 166.6 eV gradually grows during further dosing. A similar evolution can be seen for the C 1s spectra; the main peak is gaining intensity and gradually shifts toward higher binding energy. When the sample is annealed to 170 K (desorption of physisorbed C_4H_4S), the main C 1s feature shifts to a BE of ∼286 eV and a shoulder on its lower binding-energy side indicates the presence of at least two species (C_4H_4S and a small amount of C_xH_yS). A S 2p feature at 165.7 eV corresponds to chemisorbed thiophene, which is stable on the surface up to 260 K. At this point, the coverage of thiophene is at least three times bigger than that found for the C_4H_4S/ZnO system at 250 K (∼0.08 monolayer, Figures 1 and 2). Upon annealing to 350 K, the C 1s and S 2p chemisorbed thiophene features decrease indicating the removal of thiophene from the surface. Simultaneously, there is an increase of the feature of atomic sulfur at a BE of 160.5 eV. Thiophene disappears from $Cs_{0.4}$/ZnO by 500 K and mainly atomic sulfur, and a small amount of carbon residuals are left on the surface.

The behavior of thiophene on the $Cs_{0.2}$/ZnO system at 300 K is shown in Figure 10. Due to the high reactivity of Cs and the presence of thiophene in the chamber residual atmosphere the background spectra showed weak C 1s and S 2p features. The first dose of 0.5 langmuir yields S 2p features centered around 165.5 eV produced mainly by molecular thiophene. These features saturate after another dose of 1 langmuir and do not change their line shape upon further dosing of 2 and 4 langmuirs. At this stage the total sulfur coverage ($S + C_4H_4S$) is ∼ 0.3 monolayer. When similar experiments were done on a pure ZnO surface at 300 K, the amount of thiophene adsorbed was negligible (i.e. no substantial S 2p signal). In Figure 10, heating from 300 to 400 K leads to complete disappearance of the features for adsorbed thiophene, with S and C_xH_y species (not shown) remaining on the surface.

By comparing the photoemission results for adsorption of thiophene on ZnO and Cs/ZnO surfaces, we can conclude that the presence of cesium significantly enhances the adsorption energy of the molecule and favors its decomposition. The bonding of thiophene to Cs/ZnO was examined using ab initio SCF calculations and the cluster models shown in Figure 3. To model supported cesium, a Cs atom was set on the center of the hollow site formed by the Zn atoms labeled 1 in the first layer of the $Zn_{13}O_{13}$ cluster {$Cs/Zn_{13}O_{13}(0001)$ configuration}, or on the center of the hollow site formed by the O atoms labeled 1′ in the fourth layer {$Cs/Zn_{13}O_{13}(000\bar{1})$ configuration}. Estimates based on pure electrostatic interactions and a Madelung potential predict that these should be the adsorption sites of Cs on ZnO(0001)−Zn and ZnO(000$\bar{1}$)−O.[43] This also can be expected on the basis of SEXAFS studies for the K/ZnO-(000$\bar{1}$)−O system,[44] which indicate that the alkali adsorbs on the 3-fold hollow sites of the O-terminated surface that have a Zn atom underneath. The $Cs-Zn_1$ and $Cs-O_1$ distances in the

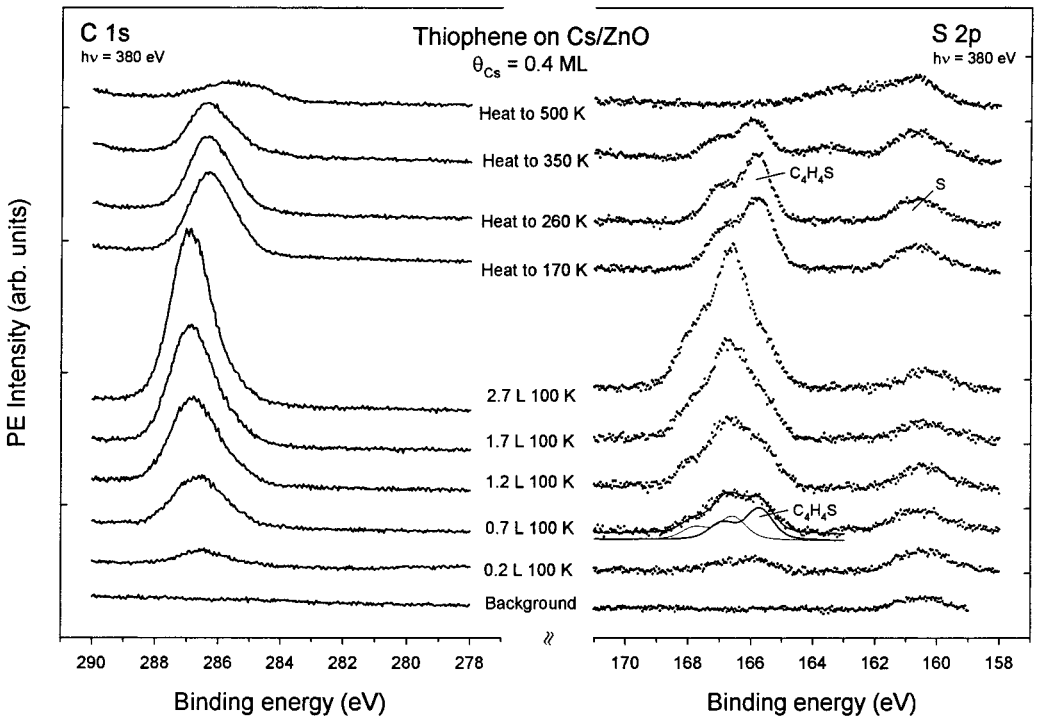

Figure 9. Carbon 1s and sulfur 2p spectra for the adsorption of thiophene on $Cs_{0.4}$/ZnO at 100 K and after annealing to 170, 260, 350, and 500 K (where ML = monolayer and L = langmuir). All the spectra were acquired in the same set of experiments using a photon energy of 380 eV.

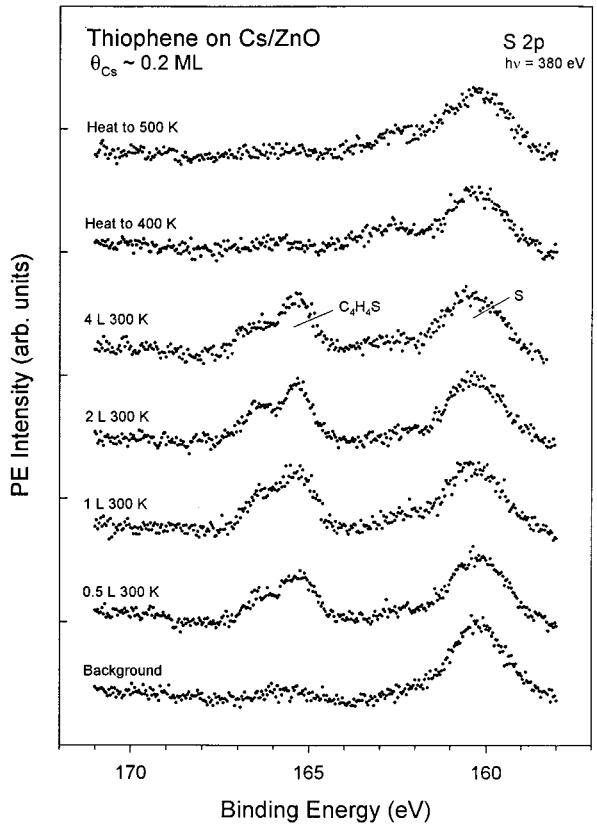

Figure 10. S 2p spectra for the adsorption of thiophene on $Cs_{0.2}$/ZnO at 300 K, followed by annealing to 400 and 500 K (where ML = monolayer and L = langmuir). All the spectra were acquired using a photon energy of 380 eV.

cluster models were optimized at the ab initio SCF level obtaining values of 3.32 and 2.97 Å, respectively. On top of the Cs adatom, thiophene was bonded with the configurations displayed at the bottom of Figure 3 and the geometry of the molecule was optimized. Table 2 lists the calculated structural parameters. For bonding through the aromatic ring, one finds significant changes in the structural geometry of the molecule that favor dissociation.

TABLE 2: Adsorption of Thiophene on $Cs/Zn_{13}O_{13}$

	ads energy[a] (kcal/mol)	bond distances (Å)				thiophene charge (e)[b]
		Cs−S	Cs−Cα	Cα−S	Cα−Cβ	
free molecule				1.78	1.34	
on $Cs/Zn_{13}O_{13}(0001)$						
S-end on Cs	11	3.39		1.79	1.34	−0.05
ring on Cs	15	3.46	3.34	1.84	1.38	−0.16
on $Cs/Zn_{13}O_{13}(000\bar{1})$						
S-end on Cs	11	3.41		1.78	1.34	0.05
ring on Cs	12	3.46	3.37	1.82	1.37	−0.09

[a] A positive value denotes an exothermic process. [b] See ref 45.

The calculations predict that Cs behaves as an electron donor on the (0001)-Zn and $(000\bar{1})$-O faces of zinc oxide.[45] But despite this, in general, the alkali metal has a big chemical affinity for thiophene and bonds the molecule stronger than the Zn atoms of ZnO (compare results in Tables 1 and 2). On the O-terminated surface of $Zn_{13}O_{13}$ the calculated positive charge[45] on the Cs adatom was 0.29e larger than on the Zn-terminated surface. This had an effect on the reactivity of the alkali metal, and on Cs/ZnO(0001) one sees thiophene adsorption energies that are larger than those on Cs/ZnO$(000\bar{1})$; see Table 2. In the Cs/ZnO system, Cs adatoms that are mainly bonded to Zn probably provide the adsorption sites for the dissociation of thiophene. These Cs adatoms have a substantial electron density and interact better with the LUMO of thiophene (C−S antibonding[28]) than Cs adatoms that are mainly bonded to O or Zn centers in pure ZnO.

IV. Discussion

IV.1. Thiophene on Clean ZnO. In many petroleum refineries, sulfur compounds are removed from oil-derived feedstocks by adsorption on a bed of zinc oxide.[1,5] The oxide has a high efficiency for the removal or decomposition of mercaptans and

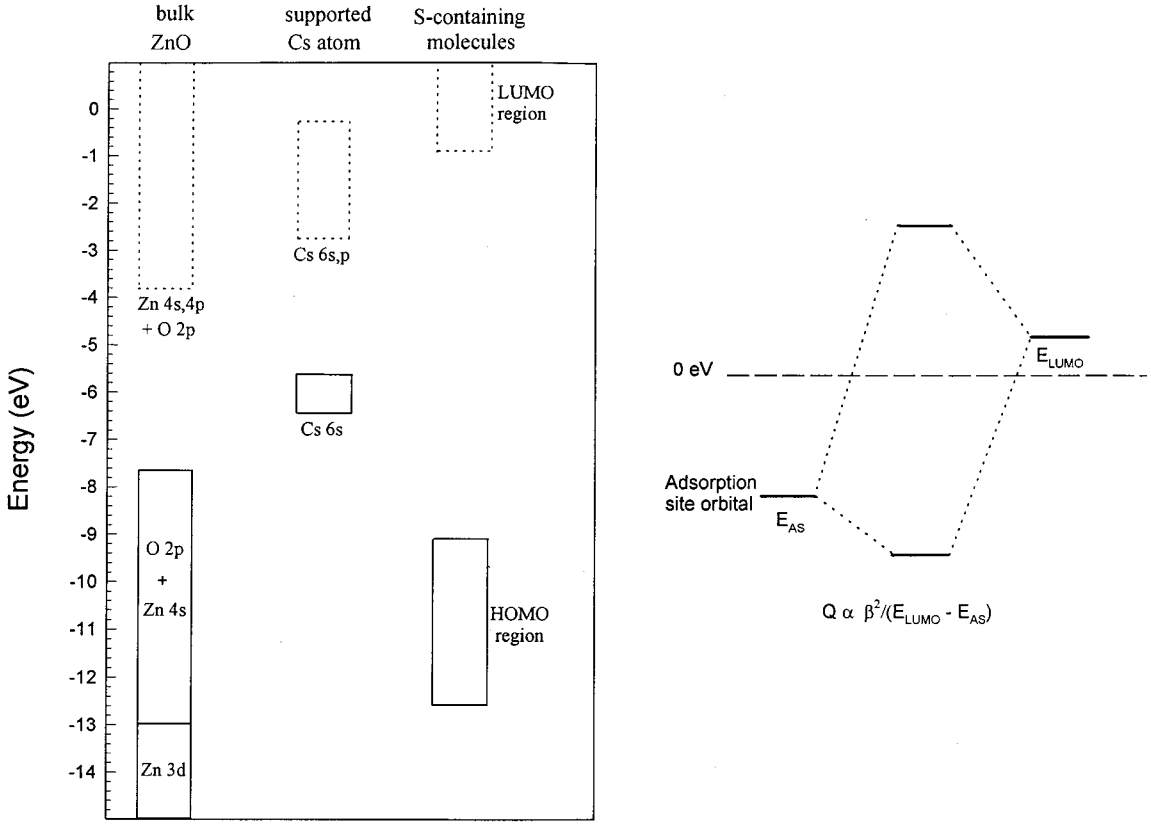

Figure 11. (Left panel) Energy range covered by the bands of ZnO.[17b,24] The empty and occupied states are indicated by dotted and solid lines, respectively. For comparison, we also show the energies for the 6s,p orbitals of a supported Cs atom on ZnO clusters[21a,27] and the typical regions in which the HOMO's and LUMO's of S-containing molecules appear.[27,28,47] All the energies are reported with respect to the vacuum level (0 of energy). (Right panel) Bonding interactions between the LUMO of a sulfur species and an occupied orbital of the adsorption site (Zn or Cs).

disulfides, but it has problems when dealing with thiophenes.[1,5] For CH_3SH on ZnO, we have found that the cleavage of the S−H bond occurs below 200 K, producing adsorbed CH_3S species that are stable up to temperatures above 400 K.[19a] ZnO exhibits a good chemical affinity for S_2,[19b] H_2S,[27] and SO_2.[21a] In contrast, the present study shows that thiophene weakly chemisorbs on clean ZnO at 100 K and most of it desorbs below 300 K. This is similar to results found on γ-Al_2O_3 where the molecule desorbs below 250 K.[17a] At saturation, three kinds of adsorbed thiophene species have been found in the C_4H_4S/γ-Al_2O_3 system: one in which the thiophene interacts weakly with hydroxyl groups (probably through hydrogen bonding), a second in which thiophene is coordinated via its sulfur atom to coordinatively unsaturated Al^{3+} sites on the surface, and a third species whose mode of adsorption is unknown.[17a] Our ab initio SCF calculations indicate that tri-coordinated Zn atoms of ZnO should bond thiophene through its S end, whereas bonding via the aromatic ring is expected for Zn atoms that have a very low coordination number. The low reactivity of thiophene on ZnO and γ-Al_2O_3 is similar to that seen on noble metals such as Ag(111)[14] and Cu(100).[16] On these noble metals, thiophene adsorbs reversibly with no other desorption products observed during thermal desorption.

IV.2. Thiophene on Metallic Cs. C_4H_4S readily decomposes on transition metal surfaces. C−S bond scission occurs below room temperature on Mo(110),[7] Ni(111),[11] Ru(001),[12] Rh(111)[13] and Pt(111).[15] The reaction products usually include hydrogen and/or hydrocarbons that desorb upon annealing to 300−500 K with atomic sulfur remaining on the surface. The reactivity of metallic cesium toward thiophene in many aspects is similar to that displayed by transition metals such as Ni, Rh, and Pt. The alkali metal exhibits an extreme chemical activity and is able to decompose C_4H_4S at very low temperatures (100 K). After elevating the temperature above 170 K, part of the adsorbed thiophene starts to desorb but a significant fraction of the adsorbed molecules undergo complete C−S bond scission by 250 K. This is consistent with the results of previous works which show that the alkali metal has a large affinity for sulfur-containing molecules: S_2,[27] H_2S,[27] SO_2,[21a] and CH_3SH.[19a] In general, these molecules partially dissociate between 100 and 200 K, and very extensive decomposition occurs upon increasing the temperature to ∼300 K. Metallic cesium has a very low work function (∼2.1 eV)[46] that makes easy the transfer of electrons from the metal surface into the vacant C−S antibonding orbitals of adsorbed organosulfur species.

IV.3. Thiophene on Cs/ZnO. When a small amount of cesium is predeposited on ZnO, one sees dramatic changes in reactivity toward thiophene. Even at low coverages of cesium (∼0.2 monolayer), there is an increase in the adsorption energy of thiophene (5−10 kcal/mol) and its rate of decomposition. This is in excellent agreement with our previous results which showed that ionic Cs ($Cs^{\delta+}$) promotes the adsorption of H_2S, S_2 and SO_2 on zinc oxide.[21,27] Thus, doping with cesium is a good route for enhancing the performance of zinc oxide as a sorbent for the removal or destruction of S-containing molecules from oil-derived feedstocks. This reflects the fact that Cs adatoms provide electronic states that are well-suited for interactions with the frontier orbitals of sulfur-containing molecules.

Figure 11 shows the energy positions for the bands in bulk ZnO,[17b,24] the 6s and 6p orbitals of a Cs atom supported on ZnO clusters,[21a,27] and the molecular orbitals of organosulfur species. In atomic Cs, the 6s orbital (at an energy of −3.4 eV [21a,27]) is only half-occupied and gets stabilized (1.8−2.3 eV)

after interacting with ZnO clusters.[21a,27] For H_2S, thiols (RSH), and thiophenic species the HOMO's appear at energies between −9 and −12 eV, with the LUMO's usually located in the range of −1 to +5 eV.[27,28,47] Following perturbation theory in combination with the Hückel and tight-binding methods,[48] one can get an approximate expression for the bonding energy (Q) derived from the interaction between the HOMO of a sulfur-containing molecule and the conduction band of an oxide:

$$Q_{\mathrm{HOMO-Cond}} \propto \beta^2_{\mathrm{HOMO-Cond}}/(E_{\mathrm{Cond}} - E_{\mathrm{HOMO}}) \qquad (1)$$

where $\beta_{\mathrm{HOMO-Cond}}$ is the resonance integral for the interacting levels and E_{Cond} and E_{HOMO} are the energies for the conduction band and HOMO, respectively. The corresponding expression for the bonding energy that arises from the hybridization of the LUMO of the sulfur-containing molecule and the valence band of the oxide is

$$Q_{\mathrm{LUMO-valence}} \propto \beta^2_{\mathrm{LUMO-valence}}/(E_{\mathrm{LUMO}} - E_{\mathrm{valence}}) \qquad (2)$$

where the $\beta_{\mathrm{LUMO-Valence}}$, E_{LUMO}, and E_{Valence} terms have a definition similar to those of the terms in eq 1. After applying eqs 1 and 2 to the systems in Figure 11, it is clear that a surface promoted with Cs offers a better energy match for the frontier orbitals of an organosulfur molecule than clean ZnO. This is particularly important for interactions with the LUMO's which are frequently C−S or S−H antibonding.[28,47]

V. Summary and Conclusions

1. On polycrystalline ZnO, the C_4H_4S molecules are weakly chemisorbed, and most of them desorb at temperatures below 300 K. A very small fraction of the adsorbed C_4H_4S (∼0.02 monolayer) that interacts with O-unsaturated Zn sites decomposes on the oxide surface.

2. S adatoms weaken the bonding interactions of thiophene on ZnO. Zinc sulfide is also considerably less reactive toward thiophene than ZnO.

3. Pure metallic Cs reacts vigorously with C_4H_4S, decomposing the molecule at very low temperatures (100−200 K). Elimination of sulfur from the thiophene ring starts between 170 and 250 K.

4. Cs adatoms enhance the adsorption energy of thiophene on ZnO by at least 5−10 kcal/mol and favor its decomposition. Results of ab initio SCF calculations indicate that the bonding interactions of thiophene with the (0001)-Zn and $(000\bar{1})$-O faces of ZnO are weak, and promotion with Cs adatoms considerably improves the energetics for C_4H_4S adsorption and C−S bond breaking. The Cs adatoms provide occupied states that are very efficient for bonding interactions with the frontier orbitals of C_4H_4S and other S-containing molecules. This should lead to an improvement in the performance of ZnO as a sorbent in desulfurization processes.

Acknowledgment. This work was carried out at Brookhaven National Laboratory and supported by the U.S. Department of Energy (Contract No. DE-AC02-98CH10886), Office of Basic Energy Sciences, Chemical Science Division. The NSLS is supported by the divisions of Materials and Chemical Sciences of the U.S. Department of Energy.

References and Notes

(1) Speight, J. G. *The Chemistry and Technology of Petroleum,* 2nd ed.; Dekker: New York, 1991.

(2) (a) Ertl, G., Knözinger, H., Weitkamp, J., Eds. *Handbook of Heterogeneous Catalysis;* Wiley-VCH: New York, 1997. (b) Bartholomew, C. H.; Agrawal, P. K.; Katzer, J. R. *Adv. Catal.* **1982**, *31*, 135. (c) Oudar, J., Wise, H., Eds. *Deactivation and Poisoning of Catalysts*; Dekker: New York, 1991.

(3) Stern, A. C.; Boubel, R. W.; Turner, D. B.; Fox, D. L. *Fundamentals of Air Pollution*, 2nd ed.; Academic Press: New York, 1984.

(4) (a) Chianelli, R. R.; Daage, M.; Ledoux, M. *Adv. Catal.* **1994**, *40*, 177. (b) Dellmon, B. *Bull. Soc. Chim. Belg.* **1995**, *104*, 173.

(5) Satterfield, C. N. *Heterogeneous Catalysis in Practice*; McGraw-Hill: New York, 1980; p 261.

(6) (a) Angelici, R. J. *Polyhedron* **1997**, *16*, 3073. (b) Wiegand, B. C.; Friend, C. M. *Chem. Rev.* **1992**, *92*, 491.

(7) (a) Zaera, F.; Kollin, E. B.; Gland, J. L. *Surf. Sci.* **1987**, *184*, 75. (b) Roberts, J. T.; Friend, C. M. *Surf. Sci.* **1987**, *186*, 201. (c) Fulmer, J. P.; Zaera, F.; Tysoe, W. T. *J. Phys. Chem.* **1988**, *92*, 4147.

(8) Preston, R. E.; Benziger, J. B. *J. Phys. Chem.* **1985**, *89*, 5010.

(9) Kelly, D. G.; Odriozola, J. A.; Somorjai, G. A. *J. Phys. Chem.* **1987**, *91*, 5695.

(10) Cheng, L.; Bocarsly, A. B.; Bernasek, S. L.; Ramanarayanan, T. A. *Surf. Sci.* **1997**, *374*, 357.

(11) Huntley, D. R.; Mullins, D. R.; Wingeier, M. P. *J. Phys. Chem.* **1996**, *100*, 19620.

(12) Heise, W. H.; Tatarchuk, B. J. *Surf. Sci.* **1989**, *207*, 297.

(13) Netzer, F. P.; Bertel, E.; Goldmann, A. *Surf. Sci.* **1988**, *201*, 257.

(14) Caldwell, T. E.; Abdelrehim, I. M.; Land, D. P. *Surf. Sci.* **1996**, *367*, L26.

(15) (a)Lang, J. F.; Masel, R. I. *Surf. Sci.* **1987**, *183*, 44. (b) Stohr, J.; Gland, J. L.; Kollin, E. B.; Koestner, R. J.; Johnson, A. L.; Muetterties, F. S., *Phys. Rev. Lett.* **1984**, *53*, 2161.

(16) (a) Sexton, B. A. *Surf. Sci.* **1985**, *163*, 99. (b) Imanishi, A.; Yokoyama, T.; Kitajima, Y.; Ohta, T. *Bull. Chem. Soc. Jpn.* **1998**, *71*, 831.

(17) (a) Quigley, W. W. C.; Yamamoto, H. D.; Aegerter, P. A.; Simpson, G. J.; Bussell, M. E. *Langmuir* **1996**, *12*, 1500. (b) Heinrich, V. E.; Cox, P. A. *The Surface Science of Metal Oxides*; Cambridge Press: New York 1994. (c) Barteau, M. A. *Chem. Rev.* **1996**, *96*, 1413.

(18) Williams, G. P. *Electron Binding Energies of the Elements*, Version II; National Synchrotron Light Source, Brookhaven National Laboratory: Upton, NY, 1992.

(19) (a) Dvorak, J.; Jirsak, T.; Rodriguez, J. A. Manuscript in preparation. (b) Chaturvedi, S.; Rodriguez, J. A.; Hrbek, J. *Surf. Sci.* **1997**, *384*, 260. (c) Rodriguez, J. A.; Hrbek, J. *J. Vac. Sci. Technol.* A **1994**, *12*, 2140.

(20) Rodriguez, J. A.; Li, S. Y.; Hrbek, J.; Huang, H. H.; Xu, G. Q. *J. Phys. Chem.* **1996**, *100*, 14476.

(21) (a) Rodriguez, J. A.; Jirsak, T.; Hrbek, J. *J. Phys. Chem. B* **1999**, *103*, 1966. (b) Chaturvedi, S.; Rodriguez, J. A. *Surf. Sci.* **1998**, *401*, 282.

(22) Heegemann, W.; Meister, K. H.; Betchtold, E.; Hayek, K. *Surf. Sci.* **1975**, *256*, 161.

(23) Xu, G. Q.; Hrbek, J. *Catal. Lett.* **1989**, *2*, 35.

(24) Chaturvedi, S.; Rodriguez, J. A.; Hrbek, J. *J. Phys. Chem B* **1997**, *101*, 10860.

(25) Hrbek, J.; van Campen, D. G.; Malik, I. J. *J. Vac. Sci. Technol.* A **1995**, *13*, 1409.

(26) Dupuis, M.; Chin, S.; Marquez, A. In *Relativistic and Electron Correlation Effects in Molecules and Clusters;* Malli, G. L., Ed.; NATO ASI Series; Plenum: New York, 1992.

(27) Rodriguez, J. A.; Jirsak, T.; Chaturvedi, S.; Hrbek, J. *Surf. Sci.* **1998**, *171*, 188.

(28) Rodriguez, J. A. *J. Phys. Chem.* **1997**, *101*, 7524.

(29) (a) Rodriguez, J. A.; Chaturvedi, S.; Kuhn, M.; Hrbek, J. *J. Phys. Chem. B* **1998**, *102*, 5511. (b) Rodriguez, J. A.; Chaturvedi, S.; Kuhn, M. *Surf. Sci.* **1998**, *415*, L1065. (c) Rodriguez, J. A.; Jirsak, T.; Chaturvedi, S.; Hrbek, J. *J. Am. Chem. Soc.* **1998**, *120*, 11149. (d) Rodriguez, J. A.; Chaturvedi, S.; Hanson, J.; Brito, J. L. *J. Phys. Chem. B* **1999**, *103*, 770.

(30) (a) Whitten, J. L.; Yang, H. *Surf. Sci. Rep.* **1996**, 24, 55. (b) van Santen, R. A.; Neurock, M. *Catal. Rev.—Sci. Eng.* **1995**, *37*, 557. (c) Freund, H.-J.; Kulenbeck, H.; Staemmler, V. *Rep. Prog. Phys.* **1996**, *59*, 283.

(31) Ruette, F., Ed. *Quantum Chemistry Approaches to Chemisorption and Heterogeneous Catalysis*; Kluwer: Dordtrecht, The Netherlands, 1992.

(32) (a) Pacchioni, G.; Ferrari, A. M.; Bagus, P. S. *Surf. Sci.* **1996**, *350*, 159. (b) Anchell, J. L.; Hess, A. C. *J. Phys. Chem.* **1996**, *100*, 18317. (c) Mejias, J. A.; Marquez, A. M.; Fernandez-Sanz, J.; Fernandez-Garcia, M.; Ricart, J. M.; Sousa, C.; Illas, F. *Surf. Sci.* **1995**, *327*, 59.

(33) Chaturvedi, S.; Rodriguez, J. A.; Jirsak, T.; Hrbek, J. *J. Phys. Chem. B* **1998**, *102*, 7033.

(34) Abrahams, S. C.; Berstein, J. L. *Acta Crystallogr. B* **1969**, *25*, 1223.

(35) Harshbarger, W. R.; Bauer, S. H. *Acta Crystallogr. B* **1970**, *26*, 1010.

(36) (a) Zonnevylle, M.; Hoffmann, R.; Harris, S. *Surf. Sci.* **1988**, *199*, 320. (b) Atencio, R.; Rincon, L.; Sanchez-Delgado, R.; Ruette, F. Submitted for publication. (c) Diemann, E.; Weber, T.; Muller, A. *J. Catal.* **1994**, *148*, 288. (d) Ruette, F.; Valencia, N.; Sanchez-Delgado, R. A. *J. Am. Chem. Soc.* **1989**, *111*, 40.

(37) Wagner, C. D.; Riggs, W. M.; Davis, L. E.; Moulder, J. F.; Muilenberg, G. E. *Handbook of X-ray Photoelectron Spectroscopy*; Perkin-Elmer: Eden Prairie, MN, 1976.

(38) Hrbek, J.; Yang, Y. W.; Rodriguez, J. A. *Surf. Sci.* **1993**, *296*, 164.

(39) Egelhoff, W. F. *Surf. Sci. Rep.* **1987**, *6*, 253.

(40) Rodriguez, J. A. *Surf. Sci.* **1992**, *278*, 326.

(41) (a) Campbell, C. T. *Surf. Sci. Rep.* **1997**, *27*, 1. (b) Madey, T.; Yakshinsky, B. V.; Ageev, V. N.; Johnson, R. E. *J. Geophys. Res.* **1998**, *103*, 5873.

(42) Chaturvedi, S.; Rodriguez, J. A. *Surf. Sci.* **1998**, *401*, 282.

(43) Leysen, R.; Hopkins, B. J.; Taylor, P. A. *J. Phys. Chem. C*: *Solid State Phys.* **1975**, *8*, 907.

(44) Purdie, D.; Muryn, C. A.; Crook, S.; Wincott, P. L.; Thorton, G.; Fischer, D. A. *Surf. Sci.* **1993**, *290*, L680.

(45) (a) The charges were calculated using a Mulliken population analysis.[45b] Due to the limitations of this type of analysis, the charges must be interpreted only in qualitative terms.[45c] (b) Mulliken, R. S. *J. Chem. Phys.* **1955**, *23*, 1841 (c) Szabo, A.; Ostlund, N. S. *Modern Quantum Chemistry*; McGraw-Hill: New York, 1989.

(46) Michaelson, H. B. *J. Appl. Phys.* **1977**, *48*, 4729.

(47) (a) Rodriguez, J. A.; Chaturvedi, S.; Kuhn, M.; van Ek, J.; Diebold, U.; Robbert, P. S.; Geisler, H.; Ventrice, C. A. *J. Chem. Phys.* **1997**, *107*, 9146. (b) Rodriguez, J. A. *Surf. Sci.* **1992**, *278*, 326.

(48) (a) Shustorovich, E.; Baetzold, R. C. *Science* **1985**, *227*, 876. (b) Hammer, B.; Morikawa, Y.; Nørkskov, J. K. *Phys. Rev. Lett.* **1996**, *76*, 2141.